Heliyon 10 (2024) e24563

Contents lists available at ScienceDirect

Heliyon

journal homepage: www.cell.com/heliyon

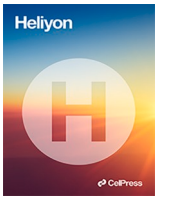

Research article

Tetraclinis articulata (Vahl) Mast.: Volatile constituents, antioxidant, antidiabetic and wound healing activities of its essential oil

Sohaib Khatib [a,b], Ismail Mahdi [b], Badreddine Drissi [a,b], Nidal Fahsi [b], Latifa Bouissane [a,**], Mansour Sobeh [b,*]

[a] *Molecular Chemistry, Materials and Catalysis Laboratory, Faculty of Sciences and Technologies, Sultan Moulay Slimane University, Beni-Mellal, Morocco*

[b] *AgroBioSciences Program, College of Agriculture and Environmental Science, Mohammed VI Polytechnic University, Ben Guerir 43150, Morocco*

A R T I C L E I N F O

Keywords:
Tetraclinis articulata
α-amylase
α-glucosidase
Tyrosinase
Elastase
Type 2 diabetes
Wound healing

A B S T R A C T

Type 2 diabetes mellitus (T2DM) is a metabolic syndrome known to contribute to impaired wound healing. This condition can be further worsened by excessive melanin production, elastin degradation, and chronic infections at the wound site, potentially leading to melasma and diabetic dermopathy. The purpose of this study was to investigate the phytochemical profile and inhibitory effects of *Tetraclinis articulata* essential oil (TAEO) on target enzymes involved in diabetes pathogenesis and chronic wound remodeling, namely *α*-amylase, *α*-glucosidase, tyrosinase, and elastase, as well as its *in vitro* antibacterial activity. Gas chromatography and mass spectrometry (GC-MS) analysis of TAEO led to the identification of 46 volatile compounds, representing 96.61 % of TAEO. The major metabolites were bornyl acetate (29.48 %), *α*-pinene (8.96 %), germacrene D (7.70 %), and D-limonene (5.90 %). TAEO exhibited limited scavenging activity against DPPH free radicals, whereas the FRAP and ABTS assays indicated a relatively higher antioxidant activity. Remarkably, TAEO disclosed a promising *in vitro* antidiabetic activity against *α*-glucosidase with an IC_{50} value of 178 ± 1.6 μg/mL, which is comparable to the standard inhibitor acarbose (IC_{50} = 143 ± 1.1 μg/mL). *In silico*, molecular docking analysis against *α*-glucosidase identified 15 compounds that interacted with the enzyme's active site, whereas skin permeability and sensitization assessments indicated that 26 out of the 44 identified volatile compounds were predicted to be free from any skin sensitivity risk. On the other hand, moderate inhibitory activity was recorded against *α*-amylase, tyrosinase, and elastase. Notably, TAEO at 5 % significantly suppressed biofilm formation by *P. aeruginosa, S. aureus*, and *E. faecalis*, common skin pathogens associated with wound infections, and reduced their swarming motility. Our findings suggest that TAEO may hold the potential as a natural remedy for type 2 diabetes and its associated co-morbidities, especially chronic wounds.

* Corresponding author.
** Corresponding author.
E-mail addresses: l.bouissane@usms.ma (L. Bouissane), mansour.sobeh@um6p.ma (M. Sobeh).

https://doi.org/10.1016/j.heliyon.2024.e24563
Received 19 July 2023; Received in revised form 16 December 2023; Accepted 10 January 2024
Available online 17 January 2024

1. Introduction

According to the World Health Organization (WHO), non-communicable chronic diseases (NCDs) pose a serious public health burden due to their high morbidity and mortality rates, accounting for 74 % of all deaths worldwide. Globally, type II diabetes mellitus (T2DM) ranks third among the leading causes of premature mortality [1]. It is a multifactorial complex disease characterized by persistent hyperglycemia, taking place when the pancreas fails to produce enough insulin (insulin secretion deficiency), or when the body ceases to utilize insulin efficiently (insulin resistance), or both [2]. T2DM occurs due to the strong influence of socio-economic inequalities and unhealthy lifestyle-related behaviors such as high Body Mass Index (BMI), obesity, smoking, and physical inactivity [3].

The inhibition of key carbohydrate-hydrolyzing enzymes such as α-glucosidase and α-amylase has been suggested as one of the therapeutic approaches to control postprandial hyperglycemia by preventing glucose absorption. The use of several synthetic anti-diabetic agents has been associated with severe adverse effects, including flatulence, vomiting, diarrhea, and abdominal cramps [4,5]. Consequently, the search for new naturally based α-amylase and α-glucosidase inhibitors devoid of hazardous side effects has been intensified during the last years.

In T2DM, poor wound healing, or diabetic wounds, is a serious complication. It affects the healing physiological phases (homeostasis, inflammation, proliferation, and remodeling), resulting in chronic wounds and higher risks of amputation and death [6,7]. These lesions are marked by excessive inflammation, with a persistent neutrophil and macrophage infiltration accompanied by increased release of pro-inflammatory cytokines, including interleukin 1β (IL-1β), interleukin 6 (IL-6), tissue necrosis factor alpha (TNF-α), and matrix metalloproteinases (MMPs). These cytokines negatively impact fibroblast migration and proliferation, extracellular matrix, collagen and elastin synthesis, and increase susceptibility to infections [8,9]. Moreover, the increased activity of tyrosinase and melanocyte leads to excessive melanin production and abnormal pigmentation at the wound site. Melanin accumulation interferes with collagen synthesis and angiogenesis, which are crucial for wound healing, leading to retarded healing and compromised tissue regeneration [10]. Elastase, an enzyme involved in elastin breakdown, leads to excessive elastin degradation within the wound area. This degradation compromises the structural integrity of the extracellular matrix, resulting in a higher susceptibility to chronic wounds [11,12].

Tetraclinis articulata (Vahl) Mast. (Fig. 1), commonly known as the *Araar* tree, *Berber thuja*, and Sandarac gum tree, is a monoecious species of coniferous trees in the *Cupressaceae* family. It is native to the mountainous regions of North Africa, mainly Morocco, Algeria, and Tunisia, with relict populations occurring in Malta and near Cartagena, Spain [13–15]. Morocco boasts the largest distribution area, covering 607,900 ha spreading across the Rif Mountains, eastern Middle Atlas, eastern Morocco, western Middle Atlas and High Atlas, valleys of the central plateau and eastern Meseta, and Anti-Atlas [13,16].

Traditionally, the leaves and aerial parts are consumed orally as a decoction and/or infusion to treat diabetes mellitus, hypertension, cough, asthma, and digestive disorders [17–19]. Moreover, several ethnopharmacological reports claimed that the infusion, decoction, and cataplasm of the aerial parts are efficacious against tuberculosis, diarrhea and infection of the urinary tract, migraine, nausea, anxiety and colon diseases [20,21]. Externally, the aerial parts of the tree are crushed and mixed with honey to create a topical ointment used for rheumatism, sciatic nerve pain, foot pain, burns, inflamed wounds, sprains, pimples, and skin problems [22,23]. Phytochemical studies revealed that the *Aârar* tree is rich in phenolic acids, flavonoids, phytosterols, terpenes, and fatty acids, among others [24–26]. These secondary metabolites are responsible for the reported antioxidant [27], antimicrobial [28], cytotoxic [24], anti-inflammatory [24], antidiabetic [29,30], antiurolithiatic [31], and neuroprotective activities [32].

The current study aimed to depict the chemical profile and the antioxidant activity of TAEO from Beni Mellal-Khenifra region. We also corroborated for the first time the ethnomedicinal usage of TAEO as an antidiabetic agent against target enzymes engaged in diabetes pathogenesis, namely α-amylase and α-glucosidase. Additionally, we explored the inhibitory activity of TAEO against target enzymes involved in chronic wounds, namely tyrosinase and elastase, as well as the antibacterial, antibiofilm and anti-swarming motility effects of TAEO against *Staphylococcus aureus*, *Pseudomonas aeruginosa*, and *Enterococcus faecalis*.

Fig. 1. Representative photos of *Tetraclinis articulata* (Vahl) Mast. 2023©.

2. Materials and methods

2.1. Plant material, essential oil extraction and GC-MS identification

Tetraclinis articulata (Vahl) Mast. leafy twigs were harvested from the Commune of Bni-Bataou (32°54′26.9″N 6°16′51.5″W), Beni Mellal-Khenifra region, Morocco, during the flowering season (April 2022). The plant's botanical name was confirmed by plant taxonomist Dr.Abdelmonaim Homrani Bakali from the regional Center of Agricultural Research of Errachidia, and a voucher number P5-501-2023 was assigned, and a sample was deposited at our lab entity. In the current study, the leafy twigs of *T. articulata* (300 g) were subjected to hydrodistillation using a Clevenger-type apparatus for 3 h, yielding 0.34 % (*V/W*) of the essential oil distinguished by its balsamic aroma and slightly pale yellowish color. The chemical composition of TAEO was analyzed using gas chromatography coupled to the mass spectrometer GCMS-TQ8040 from SHIMADZU, Japan as previously described [33].

2.2. In vitro antioxidant activity

The antioxidant potential of TAEO was evaluated using three *in vitro* methods, namely the 1,1-diphenyl-2-picrylhydrazyl (DPPH) free radicals, 2, 2'-azinobis (3-ethylbenzothiazoline-6-sulfonic acid) (ABTS), and ferric reducing antioxidant power (FRAP**)** assays according to the previously described protocols [34]. The results were expressed as IC_{50} (μg/mL) (DPPH and ABTS) and as mM $FeSO_4$/g sample (FRAP).

2.3. Enzyme inhibitory activity

2.3.1. α-Glucosidase inhibitory activity

The *in vitro* α-glucosidase inhibitory activity of TAEO was carried out according to a previously described method [35], with minor modifications. The reaction mixture containing 50 μL of the diluted TAEO (500–62.5 μg/mL) and 50 μL of α-glucosidase (1.0 U/mL) dissolved in PBS (0.02 M, pH 6.9) was added to an eppendorf tube and pre-incubated for 15 min at 37 °C. Afterward, the reaction was initiated by adding 100 μL of *p*-NPG (5 mM) as a substrate and the mixtures were incubated for 20 min at 37°C. Subsequently, 300 μL of Na_2CO_3 (0.2 M) was added to terminate the reaction. The absorbance of the released *p*-nitrophenol was monitored at 405 nm (A_{405}) using a microplate reader (FLUOstar Omega). PBS and acarbose served as the negative and positive control, respectively. Triplicates were performed for each reaction. Result values are expressed as mean and standard deviation (SD). The inhibition rate (%) was determined using formula (1):

$$\text{Inhibition rate } (\%) = \left[\left(\frac{\Delta Ac - \Delta AS}{\Delta AS}\right) \times 100\right]$$

Where ΔAs**:** ($A_{\text{Sample+ Enzyme}} - A_{\text{Sample}}$), ΔAc**:** ($A_{\text{PBS+ Enzyme}} - A_{\text{PBS}}$)

2.3.2. α-Amylase inhibitory activity

The *in vitro* inhibitory activity of TAEO against α-amylase was measured according to the standard method [36], with some modifications. First, 100 μL of TAEO or acarbose (0.125–2 mg/mL) in 20 mM potassium phosphate buffer (pH, 6.9) were premixed with 100 μL of α-amylase solution (1 U/mL in the PBS buffer) and pre-incubated at 37 °C for 20 min. Next, 100 μL of the soluble starch solution (1.0 %, w/v) was introduced into each tube as the substrate and incubated at 37 °C for 30 min. Then, 200 μL of the color reagent (DNS) (96 mM 3,5-dinitrosalicylic acid and 5.3 M sodium potassium tartrate solution in 2 M NaOH) was added to terminate the reaction. The test tubes were immersed in a boiling water bath (95 °C) for 5 min and then cooled down to room temperature. Finally, 1.5 mL of distilled water was added to the reaction mixture, and the absorbance was monitored at 540 nm using a microplate reader (FLUOstar Omega). The rate of α-amylase inhibition was calculated using formula (1).

2.3.3. Anti-tyrosinase activity

The tyrosinase inhibitory activity was performed as previously described [37]. First, 30 μL of mushroom tyrosinase solution (210 U/mL) and 70 μL of the diluted sample (0.012–3 mg/mL) were mixed in a 96-well microplate and pre-incubated for 10 min at 37 °C. Then, 110 μL of L-DOPA (1 mmol/L, for the diphenolase activity) or L-Tyrosine (0.5 mmol/L, for the monophenolase activity) was added to the mixture and incubated for 25 min at 37 °C. Kojic acid served as the positive control in the experiment, and each reaction was carried out in triplicate. The tyrosinase inhibitory activity was determined using the following formula:

$$\text{Inhibition } (\%) = \left[\left(\frac{\mathbf{A} \text{ control} - \mathbf{A} \text{ sample}}{\mathbf{A} \text{ control}}\right) \times 100\right]$$

Where, As: ($A_{\text{Sample+ Enzyme}} - A_{\text{Sample}}$), Ac: ($A_{\text{PBS+ Enzyme}} - A_{\text{PBS}}$)

2.3.4. Anti-elastase activity

The elastase inhibition assay was conducted following a slightly modified version of the method described [38]. Porcine pancreatic elastase enzyme was prepared as a stock solution with a concentration of 3.33 mg/mL in sterile water. The substrate N-Succinyl-A-la-Ala-Ala-*p*-nitroanilide (AAAPVN) was dissolved in 0.2 mM Tris–HCl buffer (pH = 8) to obtain a 1.6 mM solution. Then, 50 μL of the

sample solution (3–0.046 mg/mL), Tris–HCl buffer, and enzyme were pre-incubated for 15 min. Subsequently, 50 μL of the substrate was added to make up a final volume of 200 μL, and the reaction mixtures were incubated for 20 min at 37 °C. The absorbance values were immediately measured at 400 nm using a microplate reader (FLUOstar Omega). EGCG was used as the positive control in the experiment. The percentage of elastase inhibition (%) was calculated according to the following formula:

$$\text{Inhibition } (\%) = \left[\left(\frac{\mathbf{A}\text{ control} - \mathbf{A}\text{ sample}}{\mathbf{A}\text{ control}}\right) \times 100\right]$$

Where, **As**: The corrected absorbance of the samples ($A_{\text{Sample+ Enzyme}} - A_{\text{Sample}}$), **Ac**: The corrected absorbance of controls ($A_{\text{Buffer+Enzyme}} - A_{\text{Buffer}}$)

2.4. Antibacterial activity

2.4.1. Determination of the minimum inhibitory concentration (MIC)

The minimum inhibitory concentration (MIC) of TAEO towards *Staphylococcus aureus, Pseudomonas aeruginosa*, and *Enterococcus faecalis* was evaluated using the broth microdilution assay in a 96-well microtiter microplate [39,40]. Initially, the sample was solubilized in Muller–Hinton (MH) broth supplemented with 5 % dimethyl sulfoxide (DMSO) to achieve a final concentration of 20 %. Subsequently, the sample underwent sterilization using 0.22 μm sterile syringe filters and was then subjected to two-fold serial dilution in triplicate into the wells of the microplate (20 %–1.25 %). Next, fresh overnight suspensions of *P. aeruginosa*, *S. aureus*, and *E. faecalis* adjusted to achieve a turbidity level of $OD_{600nm} = 0.6$ were added to each well (2 μL per well). Negative control was established in wells without bacterial inoculation, and growth controls were included by using media without extract amendment. Ampicillin at concentrations ranging from 10 to 0.078125 mg/mL served as the standard antibiotic. The plate was placed in an incubator set at 37 °C with continuous shaking at 150 rpm under an aerobic environment. After incubation for 18 h, the bacterial growth was monitored visually and spectrophotometrically. The minimum inhibitory concentration was determined as the lowest concentration that prevented the bacterium's visible growth.

2.4.2. Biofilm inhibition activity using the crystal violet assay

Biofilm inhibition activity of TAEO at sub-MIC concentrations was investigated using a crystal violet (CV) colorimetric assay as previously reported [41,42]. The sample was prepared following the procedure outlined in the MIC assay. Following incubation, the bacterial suspensions were discarded, and each well was gently washed 3 times with phosphate-buffered saline (PBS, pH = 7.4) to eliminate unbound bacterial cells. Next, the bound bacteria were stained with a 1 % crystal violet (CV) solution (200 μL per well) and incubated at room temperature for 15 min. The CV solutions were disposed of, and the wells were rinsed with sterile distilled water to eliminate the excess dye. After air-drying the plate, 200 μL of 95 % ethanol was added to each well to dissolve the attached biofilm. Finally, a multimode plate reader was used to measure the biofilm amount spectrophotometrically at OD_{600nm}.

2.4.3. Swarming motility assay

The effects of TAEO at sub-MIC concentrations (1/4 and 1/8) were assessed on the *P. aeruginosa*, *S. aureus*, and *E. faecalis* swarming motility [41]. First, the swarming plate media (LB medium, 0.6 % agar) was prepared and autoclaved [43,44]. After the media had cooled to a temperature below 50 °C, they were mixed with the previously filtered EO to obtain final concentrations equivalent to 1/8 and 1/4 MIC. The plates were then allowed to dry in a laminar flow hood. Afterward, 10 μL of a fresh suspension of *S. aureus*, *P. aeruginosa*, and *E. faecalis* adjusted to $OD_{600nm} = 0.6$, was placed in the center of the agar plates and incubated at 37 °C for 24 h. The diameters of the motility zones were measured in cm.

2.5. Molecular docking and skin application

Virtual screening analyses were carried out as reportedly described [38]. Briefly, the identified volatile secondary metabolites in TAEO were docked into the binding active sites of α-Glucosidase (PDB id: 3WY1). Skin permeability, also known as log *K*p, is a parameter used to measure the rate of a chemical penetrating across the stratum corneum (SC), which is the outermost layer of the epidermis [45]. Therefore, we used the SwissADME database to determine the log *K*p values for all identified volatile compounds. Additionally, we evaluated the potential for skin sensitization among the identified compounds using the human skin sensitizer score from the SkinSens database (https://cwtung.kmu.edu.tw/skinsensdb/, accessed on June 19, 2023). This scoring system operates on a scale ranging from 0 to 1, where volatile compounds with a score of 0 are least likely to cause skin sensitization, while those with a score of 1 are most likely to induce skin sensitization. Compounds that score above a certain threshold ($\geq$0.5) are classified as skin sensitizers [46].

2.6. Statistical analysis

The experiments were carried out in triplicate, and the values are presented as means ± standard deviation (SD). To determine significant differences between group means, the Tukey's post hoc test was performed using IBM SPSS software. A *p*-value of less than 0.05 was considered statistically significant.

3. Results and discussion

3.1. Chemical composition of TAEO

The essential oil was analyzed and quantified using GC-MS analysis. Altogether, 46 compounds were identified, accounting for 96.61 % of the essential oil composition (Table 1). The oxygenated monoterpene bornyl acetate (29.48 %) was the most abundant volatile compound in the EO, followed by *α*-pinene (8.96 %), germacrene D (7.70 %), D-limonene (5.90 %), and (E)-caryophyllene (5.44 %) (Fig. 2). As shown in Table 1, oxygenated monoterpenes were the most prevalent class of volatile metabolites (33.83 %), followed by sesquiterpene hydrocarbons (27.39 %), monoterpene hydrocarbons (18.72 %), and oxygenated sesquiterpenes (9.93 %).

Our results are consistent with those of El Jemili et al. (2016), who reported bornyl acetate (26.81 %), camphor (22.40 %), *α*-pinene (7.16 %), and limonene (3.82 %) as the prevailing compounds in the essential oil of *T. articulata* aerial parts, gathered from the

Table 1
Chemical composition of the aerial parts of TAEO.

N°	Compounds	Retention index		Relative abundance (%)	Log *Kp** (cm/s)
		$RI^{A}_{Cal.}$	$RI^{B}_{Lit.}$		
1.	Tricyclene	916	926	0.50	−4.83
2.	**α-Pinene**	927	932	**8.96**	−3.95
3.	Camphene	944	954	0.55	−4.13
4.	Sabinene	965	975	0.08	−4.94
5.	*β*-Pinene	978	979	0.27	−4.18
6.	*β*-Myrcene	983	990	1.90	−4.17
7.	*p*-Cymene	1018	1024	0.27	−4.21
8.	**D-Limonene**	1024	1029	**5.90**	−3.89
9.	γ-Terpinene	1054	1053	0.39	−3.94
10.	Terpinolene	1091	1089	0.40	−3.96
11.	*α*-Campholenal	1123	1126	0.12	−5.91
12.	*trans*-Pinocarveol	1138	1139	0.15	−5.96
13.	Camphor	1144	1146	3.46	−5.67
14.	Camphene hydrate	1148	1149	0.39	−5.61
15.	Borneol	1167	1169	1.85	−5.31
16.	Terpinen-4-ol	1179	1177	0.40	−4.93
17.	*α*-Terpineol	1191	1188	0.19	−4.83
18.	(−)-Myrtenol	1199	1195	0.10	−4.94
19.	Fenchyl acetate	1223	1220	0.11	−4.84
20.	Cumin aldehyde	1245	1241	0.15	−5.52
21.	(−)-Carvone	1249	1243	0.10	−5.29
22.	2,6,11-Trimethyl-dodecane	1281	1280	0.14	−2.29
23.	**Bornyl acetate**	1288	1285	**29.48**	−4.44
24.	*α*-Terpinyl acetate	1352	1349	2.33	−4.69
25.	Copaene	1379	1376	2.10	−4.37
26.	β-Bourbonene	1388	1388	0.13	−4.20
27.	Isoledene	1396	1376	3.38	−4.66
28.	**(E)-Caryophyllene**	1421	1419	**5.44**	−4.44
29.	*α*-Humulene	1453	1454	1.63	−4.32
30.	γ-Muurolene	1472	1479	1.79	−4.49
31.	**Germacrene D**	1477	1481	**7.70**	−4.18
32.	γ-Cadinene	1509	1513	1.42	−4.49
33.	δ-Cadinene	1518	1523	3.60	−4.85
34.	Zonarene	1521	1529	0.20	−4.69
35.	Caryophyllene oxide	1589	1583	1.19	−5.12
36.	Salvial-4(14)-en-1-one	1598	1594	0.20	−5.10
37.	Aromadendrene oxide-(2)	1613	1602	0.81	−5.03
38.	1,10-di-*epi*-Cubenol	1621	1619	0.10	−5.03
39.	1-*epi*-cubenol	1636	1628	4.16	−5.03
40.	Cedrelanol	1649	1640	1.67	−5.29
41.	*α*-Cadinol	1661	1654	1.19	−5.29
42.	(6Z)-6-Pentadecen-2-one	1675	1668	0.35	−3.93
43.	Cadalin	1684	1676	0.19	−3.55
44.	Eudesma-4(15),7-dien-1β-ol	1696	1688	0.61	−5.51
45.	*n*-Eicosane	1712	–	0.61	−0.60
46.	*n*-Octadecane	1721	1800	0.14	−1.20
Monoterpene hydrocarbons				**18.72**	
Oxygenated monoterpenes				**38.83**	
Sesquiterpene hydrocarbons				**27.39**	
Oxygenated Sesquiterpenes				**9.93**	
Others				**1.74**	
Total identified components				**96.61**	

RI_{cal}: Retention indices relative to C_7–C_{40} *n*-alkanes calculated on Rtx®-5MS fused-bond column; **RI_{Lit}:** Literature retention indices [54].

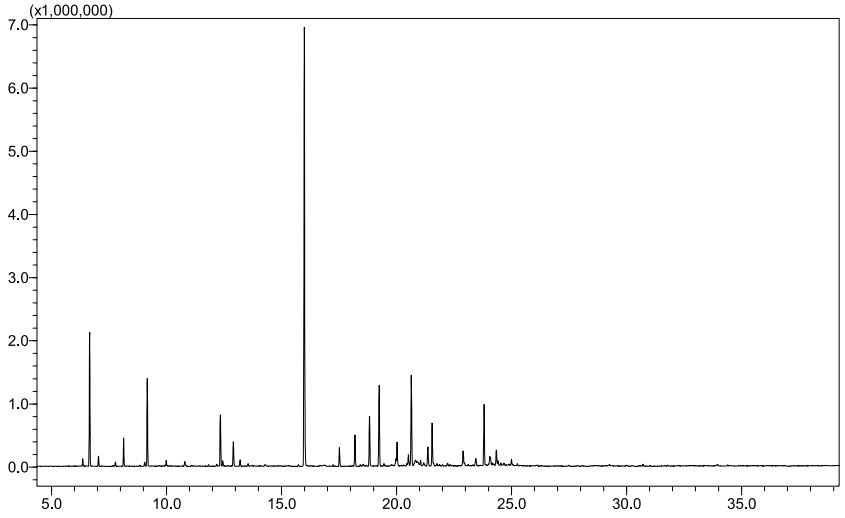

Fig. 2. GC-MS chromatogram of TAEO.

Marrakech region. Similarly, the EO of *T. articulata* leaves harvested from the Moroccan eastern region was found to be rich in monoterpene hydrocarbons and oxygenated monoterpenes, representing 47.0 % and 41.5 %, respectively. The study annotated α-pinene (22.6 %), bornyl acetate (16.8 %), camphor (14.5 %), and limonene (7.3 %) as the dominant volatile compounds, which is in accordance with our findings [32]. Similarly, the GC-MS analysis of the EO of *T. articulata* leaves from Khemisset region of Morocco afforded 34 volatile secondary metabolites dominated by bornyl acetate (30.74 %), α-pinene (23.54 %), camphor (17.27 %), and limonene (23.31 %) [47]. It should be noted, however, that our sample contained some volatile compounds that were not detected in the previous studies, especially germacrene D (7.20 %), (E)-caryophyllene (5.44 %), and 1-*epi*-cubenol (4.16 %). The occurrence of these compounds was highlighted in a study conducted in Algeria by Boussaïd et al. (2015), who asserted the presence of (E)-caryophyllene (4.7 %), germacrene D (1.1 %), and *epi*-cubenol (0.4 %) in the leaves and flowers EOs, using GC-MS and ^{13}C NMR analysis, along with the main volatile constituents α-pinene (23.6 %), bornyl acetate (20.7 %), camphor (17.3 %), and limonene (9.5 %) [48].

On the other hand, we observed that geographical provenance of the samples and the extracted organs drastically influenced the EO's chemical composition (The Moroccan and Algerian samples differ greatly from the Tunisian samples). For instance, α-pinene (56.21 %), 1,8-cineole (9.91 %), isobronyl acetate (7.46 %) were recognized as the major compounds of leaves EO from Nabeul, Tunisia [49]. Additionally, α-pinene (24.9 %), linalool acetate (21.44 %) and (E)-caryophyllene oxide (4.24 %) were highlighted as the most representative compounds of leaves EO from the region of *Cap Bon*, Tunisia [50].

While most of the previously cited studies claimed α-pinene, bornyl acetate, camphor, and limonene to be the leaves and flowers chemotaxonomic markers, El Moussaouiti et al. (2010) observed that the EO of wood burl harvested from Oulmes province of Morocco displayed a different chemical pattern with α-cedrene (22.69 %), thymol (21.59 %), and cedrenol (9.64 %) being the major constituents, whereas α-pinene, bornyl acetate, camphor, and limonene were not detected [51]. Other factors could accentuate the chemical

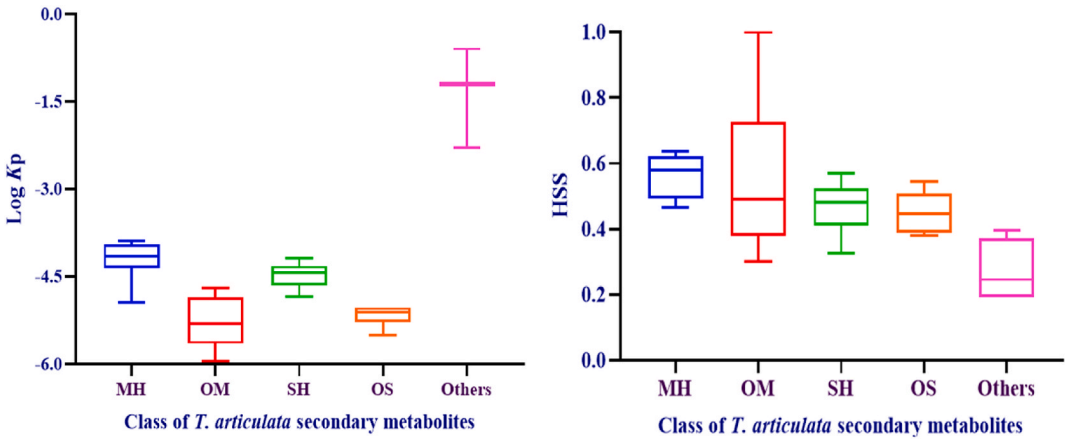

Fig. 3. Distribution of Log *K*p (Left) and human sensitizer score (HSS) (Right) according to each class of TAEO phytochemicals; abbreviation, **MH**: Monoterpene hydrocarbons, **OM**: Oxygenated monoterpenes, **SH**: Sesquiterpene hydrocarbons, **OS**: Oxygenated sesquiterpenes, **Others**: Include sesquiterpenes and alkanes, **HSS**: Human sensitizer score, **Log *Kp***: skin permeability in cm/s.

composition differences, including genetic factors, harvesting times, drying and extraction methods, and soil nutrients and their storage in the plant organs. As a result of these factors, numerous metabolic processes can take place, resulting in the synthesis of various bio-products and volatile components [52,53]. Therefore, further studies are needed to explore the relationship between these environmental and genetic factors and the chemical polymorphism within the genus.

3.2. Allergic contact dermatitis (ACD) and human sensitizer scores (HSS) of TAEO volatile metabolites

The pleasant aroma and potential therapeutic effects of TAEO render it popular to be used in topical preparations, such as ointments, creams, and perfumes, where it comes into direct contact with the skin [51]. Therefore, understanding the potential risks associated with the volatile secondary metabolites present in TAEO is crucial for ensuring the safety and efficacy of these topical products. In this context, we used the online Web tool SwissADME (http://www.swissadme.ch, accessed on May 10th, 2023) to predict the permeability of TAEO volatile metabolites through the mammalian epidermis (**Table 1**). Molecules with a more negative log *K*p are less likely to permeate the skin. We have also used the online tool (https://cwtung.nhri.edu.tw/skinsensdb/predict, accessed on May 10th, 2023) to quantitatively predict the capacity of these metabolites to induce allergic contact dermatitis (ACD) (Higher scores indicating an increased potential to cause ACD).

Altogether, the EO constituents exhibited good skin permeation, with Log *K*p values (cm/s) ranging from −0.60 to −5.96 (Fig. 3). Moreover, 18 volatile metabolites were identified as potentially sensitizer compounds representing 36.39 % of the EO chemical composition. The HSS scores varied from 0.190 to 1.00, with the highest scores achieved by (−)-carvone, *α*-campholenal, and cumin aldehyde, displaying HSS values of 1.00, 0.950, and 0.825, respectively, indicating, hence, a higher potential for allergenicity. The major volatile compound bornyl acetate has a hypoallergenic HSS score of 0.34. Other predominant VOCs, such as D-limonene, (E)-caryophyllene, and germacrene D, appear to be potential skin sensitizers, with HSS scores in the range of 0.525–0.625. Previous studies showed that some volatile metabolites such as *α*-pinene, *β*-pinene, *β*-phellandrene, and myrcene may trigger ACD through disturbing skin barrier homeostasis, increasing ROS levels, pro-inflammatory mediators such as IL-6, IL-1*β*, TNF-*α*, and NO production, and transcription factors [55–57]. However, it should be noted that the risk of developing ACD is influenced by several factors, including the individual's genetic predisposition, compound concentrations, and the route of exposure [45]. Consequently, further research is needed to draw a comprehensive insight into the potential ACD risk associated with the use of TAEO.

3.3. In vitro antioxidant activity

In the present study, the antioxidant activity of TAEO was evaluated using three *in vitro* assays, namely DPPH, ABTS, and FRAP. As shown in Table 2, the EO exhibited weak DPPH reduction activity and relatively moderate scavenging potency in the ABTS and FRAP assays. However, the obtained values remain considerably lower than those of standards, ascorbic acid and quercetin (Table 2).

The moderate antioxidant activity of TAEO could be partially attributed to the high content of bornyl acetate, *α*-pinene, germacrene D, and (*E*)-caryophyllene in the sample. The antioxidant activity of these mono- and sesquiterpenes has been reported by several previous reports [58–61]. On the other hand, the stereoselectivity of reactive species and/or the sample's solubility in various testing methods have been suggested as plausible factors altering the capacity of essential oils in quenching various radicals. Therefore, mono- and sesquiterpenes often failed to donate hydrogen atoms or are not easily soluble in the DPPH assay's reaction medium. In contrast, the ABTS and FRAP assays rely on electron transfer and are more adept at detecting the antioxidant capacity of hydrophilic, lipophilic, and highly pigmented antioxidant compounds than the DPPH assay [59,62,63].

Our findings comply with those of El Jemili et al. (2016) who used three *in vitro* assays to evaluate the antioxidant potential of the aerial parts EO of *T. articulata* collected from the Marrakech region, Morocco. The authors noticed that the EO had a poor scavenging activity towards DPPH free radicals with an IC_{50} of $12.05 \times 10^3 \pm 0.24$ μg/mL. Superior results were recorded in the ABTS and FRAP assays with IC_{50} values of $8.90 \times 10^3 \pm 0.17$ and $0.15 \times 10^3 \pm 0.01$ μg/mL, respectively [64].

In contrast to the earlier investigation, Djouahri et al. (2015) reported significant DPPH scavenging activity of the essential oil extracted from the wood and leaves collected from various locations in Algeria. The IC_{50} values varied from 88.44 ± 3.27 to 119.44 ± 5.25 μg/mL and 113.47 ± 4.19 μg/mL, respectively. The obtained values were comparable to those of BHA and BHT, with IC_{50} values of 24.73 ± 0.11 μg/mL and 33.89 ± 0.16 μg/mL, respectively [27]. The strong antioxidant could be potentially ascribed to the presence of carvacrol and thymol in the samples, which have been reported to exhibit substantial antioxidant properties [65–67]. Noteworthy, these two compounds were not detected in our sample.

Table 2
Antioxidant capacities of TAEO.

Sample/compounds	DPPH	ABTS	FRAP
	IC_{50} (μg/mL)		mM of $FeSO_4$/g Extract
TAEO	$19.8 \times 10^3 \pm 0.54$	$1.67 \times 10^3 \pm 3,1$	6.25 ± 0.09
Quercetin	5.36 ± 0.25	–	16.60 ± 0.64
Ascorbic acid	–	21.7 ± 0.29	–

3.4. Enzyme inhibitory activity

As far as we know, there have been no scientific studies dealing with the antidiabetic effects of TAEO *in vitro*. Therefore, the present study was designed to investigate the *in vitro* antidiabetic effects of TAEO on α-amylase and α-glucosidase, among others. As demonstrated in Table 3, TAEO potently inhibited α-glucosidase and moderately inhibited α-amylase in a dose dependent manner, compared to acarbose, the reference drug. In the T2DM context, the increased activity of both tyrosinase and elastase at the wound site can potentially impede the wound healing process. Therefore, we also explored the inhibitory effects of TAEO towards these target enzymes. TAEO showed moderate activity against both the monophenolase and diphenolase activities of tyrosinase. A slightly higher activity was shown against elastase; however, the obtained values remained lower than standard inhibitors Kojic acid and epigallocatechin gallate (EGCG).

The enzyme inhibitory activities could be attributed to *T. articulata* terpene-rich essential oil, especially germacrene D, terpinen-4-ol, α-pinene, 1-*epi*-cubenol, and (E)-caryophyllene. These metabolites have been suggested as potential inhibitors of these target enzymes [68,69]. The current study supports the ethnomedicinal usage of TAEO as an antidiabetic agent, suggesting that the *Aârar* tree might be a promising source for new antidiabetic agents targeting the carbohydrate metabolizing enzymes, especially α-glucosidase. Hence, this could subsequently prevent diabetic chronic wounds as one of the co-morbidities associated with T2DM.

3.5. Minimum inhibitory concentration, anti-biofilm, and anti-swarming effects of TAEO

As illustrated in Fig. 4, TAEO demonstrated a dose-dependent inhibition of *P. aeruginosa*, *S. aureus*, and *E. faecalis* growth in MH media. By monitoring the reduction of the bacterial turbidity at OD_{600}, a significant decline in bacterial growth of *P. aeruginosa* and *S. aureus* was observed starting from the concentration 1.25 % (12.5 μL/mL), with inhibition rates of 33.56 % and 23.77 %, respectively. However, the MICs values of TAEO against *P. aeruginosa*, *S. aureus*, and *E. faecalis* exceeded 20 %, indicating that complete inhibition of bacterial growth was not attained (86.48 %, 77.23 %, and 84.61 %, respectively). At a concentration of 0.3125 mg/mL, the standard antibiotic ampicillin completely inhibited the bacterial growth.

Moreover, biofilms not only enable bacterial cells to withstand antibiotics, antiseptics, and host immune responses but also contribute to the persistence of infections in chronic wounds. Therefore, we assessed the biofilm formation by *P. aeruginosa*, *S. aureus*, and *E. faecalis* in MH media supplemented with increased concentrations of TAEO. As depicted in Fig. 5, TAEO dose-dependently reduced biofilm formation by *P. aeruginosa*, *S. aureus*, and *E. faecalis*. Notably, at a concentration equivalent to 1/4 MIC (5 %), TAEO effectively decreased the amount of biofilm produced by *P. aeruginosa* and *E. faecalis* by 72.29 % and 77.26 % respectively, while *S. aureus* showed a reduction of 27.22 %.

The observed anti-biofilm activity of TAEO against these target bacteria could be potentially attributed to the permeation capacity of oxygenated monoterpenes (38.83 %) to disrupt crucial stages in the biofilm formation process, including the production of adhesion proteins and the disruption of the exopolysaccharide matrix (EPS) of the bacterial biofilm [70]. Previous studies have attributed similar antibiofilm effects to the significant presence of oxygenated monoterpenes in essential oils, such as those derived from *Backhousia citriodora* [71], *Thymus vulgaris* L. [72], and *Cymbopogon flexuosus* [73].

The swarming motility of *P. aeruginosa*, *S. aureus*, and *E. faecalis*, which is one of the critical mechanisms that enable pathogens to glide over surfaces during infections, was observed on agar plates supplemented with 1/8 and 1/4 MICs. As demonstrated in Fig. 6, TAEO showed no significant inhibition on the swarming motility of *P. aeruginosa* at the concentration equivalent to 2.5 %. However, at 5 %, TAEO decreased the swarming motility of *P. aeruginosa* by 48 %. On the other hand, *S. aureus* and *E. faecalis* were the most susceptible to TAEO, which significantly reduced their swarming motility at both 1/8 and 1/4 MICs in a dose-dependent manner.

3.6. Molecular docking

In the current study, we evaluated the *in vitro* antidiabetic and wound healing activities of TAEO against target enzymes known to be involved in diabetes pathogenesis and chronic wound healing, namely α-amylase, α-glucosidase, tyrosinase, and elastase (Table 3). The best inhibitory activity was shown on α-glucosidase with an IC_{50} value of 178 ± 1.6 μg/mL, which is comparable to the reference drug acarbose (IC_{50} = 143 ± 1.1 μg/mL). Therefore, we relied on molecular docking to gain further insight into the binding affinity of the identified volatile compounds from TAEO against α-glucosidase. Results from molecular docking revealed that fifteen out of the

Table 3
In vitro enzyme activities of the aerial parts of TAEO.

Sample/compounds	IC_{50} (μg/mL)				
	α-Amylase	α-Glucosidase	Tyrosinase		Elastase
			L-Dopa	L-Tyrosine	
TAEO	858 ± 2.67	178 ± 1.6	944.9 ± 3.11	991.5 ± 1.16	860 ± 2.7
Acarbose	267 ± 0.47	143 ± 1.1	–	–	–
Kojic acid	–	–	18.07 ± 1.08	12.52 ± 1.13	–
Quercetin	–	–	–	–	–
EGCG[a]	–	–	–	–	92.00 ± 3.1

[a] EGCG: epigallocatechin gallate.

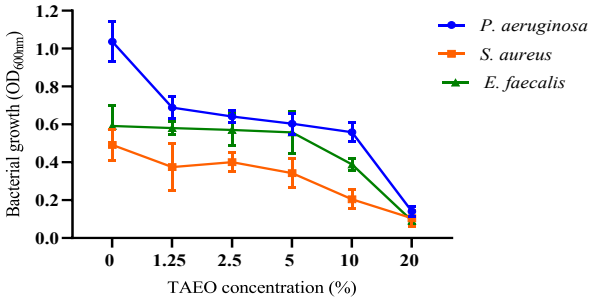

Fig. 4. The effect of TAEO on the bacterial growth of *P. aeruginosa*, *S. aureus*, and *E. faecalis*.

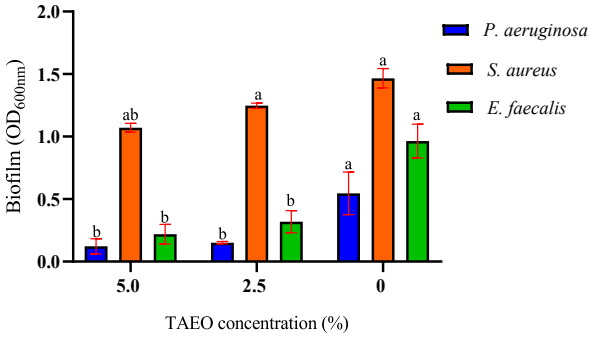

Fig. 5. Biofilm formation by *P. aeruginosa*, *S. aureus*, and *E. faecalis* cultured in the absence (0 %) and in the presence of varying concentrations of TAEO. Different superscripts indicate a statistically significant difference at 95 %.

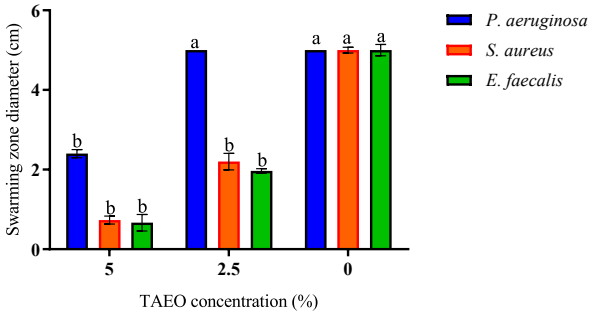

Fig. 6. Impact of TAEO sub-MICs on the swarming motility of *P. aeruginosa*, *S. aureus*, and *E. faecalis*. Different superscripts indicate a statistically significant difference at 95 %.

forty-six docked metabolites were able to interact with the active site of the enzyme, displaying scoring functions ranging from −4.97 to −8.22 kcal/mol (Table 4). These metabolites represent 16.01 % of TAEO composition, suggesting that the *in vitro* antidiabetic activity of TAEO may be mediated by these minor compounds.

The co-crystallized ligand, α-terpineol, exhibited the strongest binding at the active site, forming hydrogen bond interactions with the amino acid residues Asp 62, Arg 400 (Fig. 7). Additionally, the α-terpinyl acetate (−6.75 kcal/mol) and (6Z)-6-pentadecen-2-one (−8.22 kcal/mol) demonstrated the best docking scores, surpassing the inhibitor acarbose (−6.80 kcal/mol). Notably, (6Z)-6-pentadecen-2-one afforded hydrogen bond interactions with the amino acid residues Arg 400, as well as noncovalent pi interactions with Phe 166, whereas α-terpinyl acetate exhibited hydrophobic interactions with the amino acid residues Arg 400 and noncovalent pi interactions with Phe 166.

4. Conclusion and perspectives

The current study provides insights into the phytochemical profile and inhibitory activity of TAEO against enzymes involved in diabetes and wound healing, namely α-amylase, α-glucosidase, tyrosinase, and elastase and its antibacterial activity against *P. aeruginosa, S. aureus*, and *E. faecalis*, common skin pathogens associated with chronic wounds. GC-MS analysis identified 46 volatile

Table 4
Docking of the volatile compounds identified in TAEO against α-Glucosidase (3WY1).

Compounds	α-Glucosidase (3WY1)	
	Docking score (Kcal/mol)	Interactions
trans-Pinocarveol	−5.30	Gly 228 (Backbone donor interaction)
Camphene hydrate	−5.13	Glu 271 (H-bond)
Terpinen-4-ol	−5.97	Glu 271 (H-bond)
(−)-Myrtenol	−5.83	Asp 202 (H-bond)
Fenchyl acetate	−5.74	Arg 200 (H-bond), Asp 333 (H-bond)
Cumin aldehyde	−5.54	Arg 400 (H-bond)
(−)-Carvone	−5.72	Arg 400 (H-bond)
α-Terpinyl acetate	−6.75	Arg 400 (H-bond), Phe 166 (Hydrophobic interaction)
(E)-Caryophyllene	−4.97	Tyr 65 (Hydrophobic interaction)
γ-Cadinene	−5.28	Phe 166 (Hydrophobic interaction)
Aromadendrene oxide-(2)	−5.53	Arg 400 (H-bond)
1,10-di-*epi*-Cubenol	−5.01	Glu 271 (H-bond)
1-*epi*-Cubenol	−6.15	Gly 228 (Backbone donor interaction)
(6Z)-6-Pentadecen-2-one	−8.22	Phe 166 (Hydrophobic interaction), Arg 400 (H-bond)
α-Terpineol	−5.94	Asp 62 (H-bond), Arg 400 (H-bond)
Acarbose	−6.60	Arg 400 (H-bond), Glu 271 (H-bond), Glu 272 (Hydrophobic interaction), Asp 62 (H-bond)

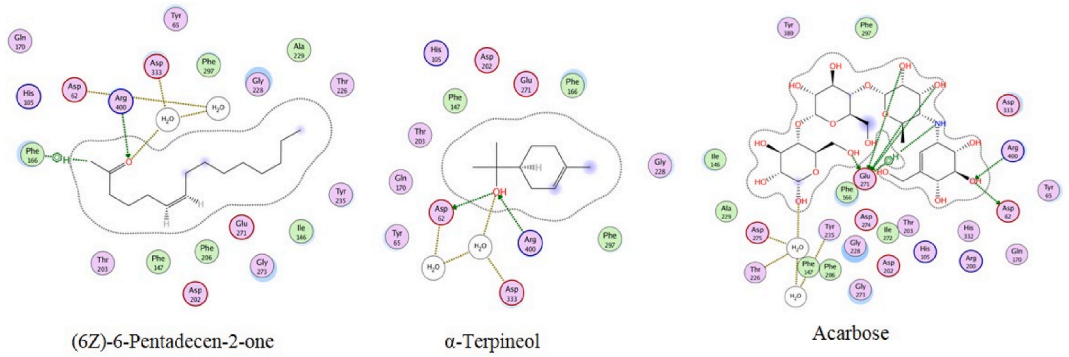

Fig. 7. 2D-interaction of some TAEO volatile compounds and the standard acarbose with amino acid residues of α-glucosidase.

compounds, representing 96.61 % of the total oil, with the main metabolites being bornyl acetate, α-pinene, germacrene D, D-limonene, and (E)-caryophyllene. TAEO had poor scavenging activity against DPPH free radicals but exhibited moderate antioxidant activity in FRAP and ABTS assays. Notably, TAEO showed promising *in vitro* antidiabetic activity against α-glucosidase. Molecular docking analysis against α-glucosidase identified 15 compounds that interact with the enzyme's active site through hydrogen bonds and noncovalent pi interactions. This suggests that these minor compounds may play a significant role in the *in vitro* antidiabetic activity of TAEO. Moreover, at 5 %, TAEO significantly decreased biofilm formation and swarming motility of *P. aeruginosa*, *S. aureus*, and *E. faecalis*. Our findings suggest that TAEO may hold versatile potential against both type 2 diabetes and chronic wounds by targeting the aforementioned enzymes and wound pathogenic bacteria. Considering these findings, further studies are needed to investigate the allergenicity of TAEO and evaluate its potential wound healing via *in vivo* models, as well as against other target enzymes involved in diabetes pathogenesis, such as DPP-4 and PTP1B.

CRediT authorship contribution statement

Sohaib Khatib: Writing – original draft, Methodology, Investigation. **Ismail Mahdi:** Writing – review & editing, Software, Investigation. **Badreddine Drissi:** Investigation. **Nidal Fahsi:** Investigation. **Latifa Bouissane:** Writing – review & editing, Supervision. **Mansour Sobeh:** Writing – review & editing, Validation, Supervision, Resources, Conceptualization.

Declaration of competing interest

The authors declare that they have no known competing financial interests or personal relationships that could have appeared to influence the work reported in this paper.

Acknowledgments

We extend our gratitude to Sultan Moulay Slimane University, Beni-Mellal, and Mohammed VI Polytechnic University, Benguerir, Morocco, for the partial support of this work.

References

[1] M. Radünz, T. Mota Camargo, H.C. dos Santos Hackbart, P. Inchauspe Correa Alves, A.L. Radünz, E. Avila Gandra, E. da Rosa Zavareze, Chemical composition and in vitro antioxidant and antihyperglycemic activities of clove, thyme, oregano, and sweet orange essential oils, LWT 138 (2021) 110632, https://doi.org/10.1016/j.lwt.2020.110632.
[2] N. Tai, F.S. Wong, L. Wen, The role of gut microbiota in the development of type 1, type 2 diabetes mellitus and obesity, Rev. Endocr. Metab. Disord. 16 (2015) 55–65, https://doi.org/10.1007/s11154-015-9309-0.
[3] K. Suwannaphant, W. Laohasiriwong, N. Puttanapong, J. Saengsuwan, T. Phajan, Association between socioeconomic status and diabetes mellitus: the national socioeconomics survey, 2010 and 2012, J. Clin. Diagn. Res. JCDR. 11 (2017) LC18–LC22, https://doi.org/10.7860/JCDR/2017/28221.10286.
[4] K. Majouli, M. Besbes Hlila, A. Hamdi, G. Flamini, H. Ben Jannet, A. Kenani, Antioxidant activity and α-glucosidase inhibition by essential oils from Hertia cheirifolia (L.), Ind. Crops Prod. 82 (2016) 23–28, https://doi.org/10.1016/j.indcrop.2015.12.015.
[5] T.K. Nguyen, L.T.T. Tran, D.H. Viet, P.H. Thai, T.P. Ha, P.V. Ty, L.P. Duc, D.T.T. Huu, L.C.V. Cuong, Xanthine oxidase, α-glucosidase and α-amylase inhibitory activities of the essential oil from Piper lolot: in vitro and in silico studies, Heliyon 9 (2023), https://doi.org/10.1016/j.heliyon.2023.e19148.
[6] M. Asif, M. Zafar, M. Saleem, M. Saadullah, S.H. Khalid, M.S.S. Khan, Mahrukh, Z. Iqbal, I.U. Khan, L. Hussain, H.S. Yaseen, H.M. Zubair, Evaluation of antidiabetic and wound healing properties of ethanol extract of Hedera nepalensis in alloxan-induced diabetic rats, South Afr. J. Bot. 146 (2022) 118–126, https://doi.org/10.1016/j.sajb.2021.10.007.
[7] J.B. Acosta, D.G. del Barco, D.C. Vera, W. Savigne, P. Lopez-Saura, G. Guillen Nieto, G.S. Schultz, The pro-inflammatory environment in recalcitrant diabetic foot wounds, Int. Wound J. 5 (2008) 530–539, https://doi.org/10.1111/j.1742-481X.2008.00457.x.
[8] M.J. Portou, R. Yu, D. Baker, S. Xu, D. Abraham, J. Tsui, Hyperglycaemia and ischaemia impair wound healing via toll-like receptor 4 pathway activation in vitro and in an experimental murine model, Eur. J. Vasc. Endovasc. Surg. Off. J. Eur. Soc. Vasc. Surg. 59 (2020) 117–127, https://doi.org/10.1016/j.ejvs.2019.06.018.
[9] M. Duff, O. Demidova, S. Blackburn, J. Shubrook, Cutaneous manifestations of diabetes mellitus, Clin. Diabetes Publ. Am. Diabetes Assoc. 33 (2015) 40–48, https://doi.org/10.2337/diaclin.33.1.40.
[10] M. Lause, A. Kamboj, E. Fernandez Faith, Dermatologic manifestations of endocrine disorders, Transl. Pediatr. 6 (2017) 300–312, https://doi.org/10.21037/tp.2017.09.08.
[11] A. Heinz, Elastases and elastokines: elastin degradation and its significance in health and disease, Crit. Rev. Biochem. Mol. Biol. 55 (2020) 252–273, https://doi.org/10.1080/10409238.2020.1768208.
[12] J.E.S. Sutcliffe, C. Thrasivoulou, T.E. Serena, L. Madden, T. Richards, A.R.J. Phillips, D.L. Becker, Changes in the extracellular matrix surrounding human chronic wounds revealed by 2-photon imaging, Int. Wound J. 14 (2017) 1225–1236, https://doi.org/10.1111/iwj.12789.
[13] V. Rozas, A.I. García-Cervigón, M. García-Hidalgo, E. Rodríguez-García, J.M. Olano, Living on the edge: legacy of water availability on Tetraclinis articulata secondary growth under semiarid conditions in Morocco, Dendrochronologia 68 (2021) 125853, https://doi.org/10.1016/j.dendro.2021.125853.
[14] S. Khatib, M. Sobeh, L. Bouissane, Tetraclinis articulata (vahl) masters: an insight into its ethnobotany, phytochemistry, toxicity, biocide and therapeutic merits, Front. Pharmacol. 13 (2022). https://www.frontiersin.org/articles/10.3389/fphar.2022.977726. (Accessed 17 November 2022).
[15] H. Harouak, J. Ibijbijen, L. Nassiri, Chemical profile of Tetraclinis articulata (Vahl) Masters, and Juglans regia L. and Olea europaea L. var. Sylvestris used against oral diseases: in vitro analysis between polyphenolic content and aqueous extraction optimization, Heliyon 7 (2021) e07118, https://doi.org/10.1016/j.heliyon.2021.e07118.
[16] F. Charrier - El Bouhtoury, A. Hakam, A. Famiri, M. Ziani, B. Charrier, Wood Characterization of Tetraclinas Articulata and Evaluation of its Resistance against Lignilolytic Fungi, 2009.
[17] M. Hachi, B. Ouafae, T. Hachi, E.B. Mohamed, B. Imane, R. Atmane, L. Zidane, Contribution to the ethnobotanical study of antidiabetic medicinal plants of the Central Middle Atlas region (Morocco), Lazaroa 37 (2016) 135–144, https://doi.org/10.5209/LAZAROA.51854.
[18] E. Idm'hand, F. Msanda, K. Cherifi, Ethnopharmacological review of medicinal plants used to manage diabetes in Morocco, Clin. Phytoscience. 6 (2020) 18, https://doi.org/10.1186/s40816-020-00166-z.
[19] M. Laadim, O. Moulay, L. Zidane, A. Hessni, O. Ali, A. M, Ethnopharmacological survey of plants used for the treatment of diabetes in the town of Sidi Slimane (Morocco), J. Pharmacogn. Phytotherapy 9 (2017) 101–110, https://doi.org/10.5897/JPP2016.0437.
[20] F. Senouci, A. Ababou, M. Chouieb, M. Chouieb, Ethnobotanical survey of the medicinal plants used in the southern Mediterranean. Case study: the region of Bissa (Northeastern Dahra Mountains, Algeria), Pharm. J. 11 (2019) 647–659, https://doi.org/10.5530/pj.2019.11.103.
[21] N. Belkacem, H. Okkacha, B. Maamar, E. Tir, Inventory, diversity and therapeutic uses of medicinal plants in the Tiaret Mountains (western Algeria), Biodiversity J. 12 (2021), https://doi.org/10.31396/Biodiv.Jour.2021.12.1.129.138.
[22] F. Jamila, E. Mostafa, Ethnobotanical survey of medicinal plants used by people in Oriental Morocco to manage various ailments, J. Ethnopharmacol. 154 (2014) 76–87, https://doi.org/10.1016/j.jep.2014.03.016.
[23] L. Viegi, K. Ghedira, Preliminary study of plants used in Ethnoveterinary Medicine in Tunisia and in Italy, Afr. J. Tradit., Complementary Altern. Med. 11 (2014) 189–199.
[24] W. Rached, F.Z. Zeghada, M. Bennaceur, L. Barros, R.C. Calhelha, S. Heleno, M.J. Alves, A.M. Carvalho, A. Marouf, I.C.F.R. Ferreira, Phytochemical analysis and assessment of antioxidant, antimicrobial, anti-inflammatory and cytotoxic properties of Tetraclinis articulata (Vahl) Masters leaves, Ind. Crops Prod. 112 (2018) 460–466, https://doi.org/10.1016/j.indcrop.2017.12.037.
[25] A. Djouahri, B. Saka, L. Boudarene, F. Benseradj, S. Aberrane, S. Aitmoussa, C. Chelghoum, L. Lamari, N. Sabaou, A. Baaliouamer, In vitro synergistic/antagonistic antibacterial and anti-inflammatory effect of various extracts/essential oil from cones of Tetraclinis articulata (Vahl) Masters with antibiotic and anti-inflammatory agents, Ind. Crops Prod. 56 (2014) 60–66, https://doi.org/10.1016/j.indcrop.2014.02.035.
[26] S. Jlizi, A. Lahmar, A. Zardi-Bergaoui, R. Ascrizzi, G. Flamini, A.H. Harrath, L. Chekir-Ghedira, H. Ben Jannet, Chemical composition and cytotoxic activity of the fractionated trunk bark essential oil from Tetraclinis articulata (vahl) Mast. Growing in Tunisia, Molecules 26 (2021) 1110, https://doi.org/10.3390/molecules26041110.
[27] A. Djouahri, S. Boualem, L. Boudarene, A. Baaliouamer, Geographic's variation impact on chemical composition, antioxidant and anti-inflammatory activities of essential oils from wood and leaves of Tetraclinis articulata (Vahl) Masters, Ind. Crops Prod. 63 (2015) 138–146, https://doi.org/10.1016/j.indcrop.2014.10.018.
[28] H. Rabib, C. Elagdi, M. Hsaine, H. Fougrach, T. Koussa, W. Badri, Antioxidant and antibacterial activities of the essential oil of Moroccan Tetraclinis articulata (vahl) masters, Biochem. Res. Int. 2020 (2020) e9638548, https://doi.org/10.1155/2020/9638548.
[29] I. Bouadid, M. Akdad, M. Eddouks, Antihyperglycemic effect of aqueous extract of Tetraclinis articulata in streptozotocin-induced diabetic rats and acute toxicity analysis, Cardiovasc. Haematol. Disord. - Drug Targetsrug Targets - Cardiovasc. Hematol. Disord. 22 (2022) 168–178, https://doi.org/10.2174/1871529X22666220908104724.
[30] M.N. Toumi, M.A. Bouzidi, A. Benyamina, A. Tilmatine, A. Megharbi, F. Toumi, Plantes agissant sur l'alpha-amylase : trigonella foenum-graecum et Tetraclinis articulata, Phytothérapie 20 (2022) 143–149, https://doi.org/10.3166/phyto-2022-0310.

[31] M. Beghalia, S. Ghalem, H. Allali, A. Belouatek, A. Marouf, Effect of herbal extracts of Tetraclinis articulata and chamaerops humilis on calcium oxalate crystals in vitro, Gomal J. Med. Sci. 5 (2007). http://www.gjms.com.pk/index.php/journal/article/view/110. (Accessed 24 May 2023).

[32] F.Z. Sadiki, M.E. Idrissi, O. Cioanca, A. Trifan, M. Hancianu, L. Hritcu, P.A. Postu, Tetraclinis articulata essential oil mitigates cognitive deficits and brain oxidative stress in an Alzheimer's disease amyloidosis model, Phytomedicine Int. J. Phytother. Phytopharm. 56 (2019) 57–63, https://doi.org/10.1016/j.phymed.2018.10.032.

[33] M.F. Mahmoud, R.A. Elrashidy, H.O. Mohammed, B. Drissi, I. Mahdi, M. Sobeh, Essential oil and polyphenolics from Thymus satureioides Coss. counteract acrylamide-induced liver toxicity through suppression of NLRP3 inflammasome/NF-κB axis, J. Funct.Foods 107 (2023) 105641, https://doi.org/10.1016/j.jff.2023.105641.

[34] N. Tawfeek, E. Fikry, I. Mahdi, M.A. Ochieng, W.B. Bakrim, N. Taarji, M.F. Mahmoud, M. Sobeh, Cupressus arizonica greene: phytochemical profile and cosmeceutical and dermatological properties of its leaf extracts, Molecules 28 (2023) 1036, https://doi.org/10.3390/molecules28031036.

[35] S. Li, R. Wang, X. Hu, C. Li, L. Wang, Bio-affinity ultra-filtration combined with HPLC-ESI-qTOF-MS/MS for screening potential α-glucosidase inhibitors from Cerasus humilis (Bge.) Sok. leaf-tea and in silico analysis, Food Chem. 373 (2022) 131528, https://doi.org/10.1016/j.foodchem.2021.131528.

[36] H.-Q. Dong, M. Li, F. Zhu, F.-L. Liu, J.-B. Huang, Inhibitory potential of trilobatin from Lithocarpus polystachyus Rehd against α-glucosidase and α-amylase linked to type 2 diabetes, Food Chem. 130 (2012) 261–266, https://doi.org/10.1016/j.foodchem.2011.07.030.

[37] M.E. Chiari, M.B. Joray, G. Ruiz, S.M. Palacios, M.C. Carpinella, Tyrosinase inhibitory activity of native plants from central Argentina: isolation of an active principle from Lithrea molleoides, Food Chem. 120 (2010) 10–14, https://doi.org/10.1016/j.foodchem.2009.09.061.

[38] A.M. Elgamal, M.A. El Raey, A. Gaara, M.A.O. Abdelfattah, M. Sobeh, Phytochemical profiling and anti-aging activities of Euphorbia retusa extract: in silico and in vitro studies, Arab. J. Chem. 14 (2021) 103159, https://doi.org/10.1016/j.arabjc.2021.103159.

[39] H.A. Abbas, A.M. Elsherbini, M.A. Shaldam, Repurposing metformin as a quorum sensing inhibitor in Pseudomonas aeruginosa, Afr. Health Sci. 17 (2017) 808, https://doi.org/10.4314/ahs.v17i3.24.

[40] W.B. Bakrim, A.D.R. Nurcahyanti, M. Dmirieh, I. Mahdi, A.M. Elgamal, M.A. El Raey, M. Wink, M. Sobeh, Phytochemical profiling of the leaf extract of ximenia americana var. caffra and its antioxidant, antibacterial, and antiaging activities in vitro and in Caenorhabditis elegans: a cosmeceutical and dermatological approach, Oxid. Med. Cell. Longev. 2022 (2022) e3486257, https://doi.org/10.1155/2022/3486257.

[41] I. Mostafa, H.A. Abbas, M.L. Ashour, A. Yasri, A.M. El-Shazly, M. Wink, M. Sobeh, Polyphenols from salix tetrasperma impair virulence and inhibit quorum sensing of Pseudomonas aeruginosa, Mol. Basel Switz. 25 (2020) 1341, https://doi.org/10.3390/molecules25061341.

[42] S. Pipattanachat, J. Qin, D. Rokaya, P. Thanyasrisung, V. Srimaneepong, Biofilm inhibition and bactericidal activity of NiTi alloy coated with graphene oxide/silver nanoparticles via electrophoretic deposition, Sci. Rep. 11 (2021) 1–9, https://doi.org/10.1038/s41598-021-92340-7.

[43] D.C. Rajapaksha, S.L. Edirisinghe, C. Nikapitiya, I. Whang, M. De Zoysa, The antimicrobial peptide octopromycin suppresses biofilm formation and quorum sensing in acinetobacter baumannii, Antibiotics 12 (2023) 623, https://doi.org/10.3390/antibiotics12030623.

[44] A.T.Y. Yeung, E.C.W. Torfs, F. Jamshidi, M. Bains, I. Wiegand, R.E.W. Hancock, J. Overhage, Swarming of Pseudomonas aeruginosa is controlled by a broad spectrum of transcriptional regulators, including MetR, J. Bacteriol. 191 (2009) 5592–5602, https://doi.org/10.1128/JB.00157-09.

[45] C. J, E. A, A. Lt, L. B, R. B, J. B, S. B, D. B, A. B, S. C, C. Mtd, I. C, C. Kp, T. D, T. E, D. F, F. Im, M. F, G. Sc, V. G, A. G, S. G, B. H, C. H, J. H, R. J, E. K, L. L, J. M, J. M, L. M, S. M, W. M, L. N, R. P, A. P, P. P, A. P, At P, R. Dw, H. S, R. S, R.D. S, S. Dt, T. Rr, D. U, A. V, B. W, T. W, At W, J. W, J. W, D. W, C. Z, Gj M, Skin sensitization in silico protocol, Regul. Toxicol. Pharmacol. RTP. 116 (2020), https://doi.org/10.1016/j.yrtph.2020.104688.

[46] I. Mahdi, N. Fahsi, H. Annaz, B. Drissi, M. Barakate, M.F. Mahmoud, M. Sobeh, Thymus satureioides coss.: mineral composition, nutritional value, phytochemical profiling, and dermatological properties, Molecules 28 (2023) 4636, https://doi.org/10.3390/molecules28124636.

[47] M. Bourkhiss, M. Hnach, B. Bourkhiss, M. Ouhssine, A. Chaouch, Composition chimique et propriétés antimicrobiennes de l'huile essentielle extraite des feuilles de Tetraclinis articulata (Vahl) du Maroc, Afr. Sci. Rev. Int. Sci. Technol. 3 (2007), https://doi.org/10.4314/afsci.v3i2.61267.

[48] M. Boussaïd, C. Bekhechi, F. Beddou, D.C. Sari, A. Bighelli, J. Casanova, F. Tomi, Chemical variability of the essential oil isolated from aerial parts of Tetraclinis articulata from North-western Algeria, Nat. Prod. Commun. 10 (2015) 1934578X1501000834, https://doi.org/10.1177/1934578X1501000834.

[49] A. Ben Ghnaya, I. Amri, M. Hanana, S. Gargouri, B. Jamoussi, A. Romane, L. Hamrouni, Tetraclinis articulata (Vahl.) Masters essential oil from Tunisia: chemical characterization and herbicidal and antifungal activities assessment, Ind. Crops Prod. 83 (2016) 113–117, https://doi.org/10.1016/j.indcrop.2015.12.026.

[50] N. Herzi, J. Bouajila, S. Camy, M. Romdhane, J.-S. Condoret, Comparison of different methods for extraction from Tetraclinis articulata: yield, chemical composition and antioxidant activity, Food Chem. 141 (2013) 3537–3545, https://doi.org/10.1016/j.foodchem.2013.06.065.

[51] M. El Moussaouiti, A. Talbaoui, S. Gmouh, M. Aberchane, A. Benjouad, Y. Bakri, D.P. Kamdem, Chemical composition and bactericidal evaluation of essential oil of Tetraclinis articulata burl wood from Morocco, J. Indian Acad. Wood Sci. 7 (2010) 14–18, https://doi.org/10.1007/s13196-010-0003-2.

[52] A. Ben Ghnaya, I. Amri, M. Hanana, S. Gargouri, B. Jamoussi, A. Romane, L. Hamrouni, Tetraclinis articulata (Vahl.) Masters essential oil from Tunisia: chemical characterization and herbicidal and antifungal activities assessment, Ind. Crops Prod. 83 (2016) 113–117, https://doi.org/10.1016/j.indcrop.2015.12.026.

[53] M. Sobeh, M.S. Braun, S. Krstin, F.S. Youssef, M.L. Ashour, M. Wink, Chemical profiling of the essential oils of Syzygium aqueum, Syzygium samarangense and Eugenia uniflora and their discrimination using chemometric analysis, Chem. Biodivers. 13 (2016) 1537–1550, https://doi.org/10.1002/cbdv.201600089.

[54] R. Adams, Identification of essential oil components by gas chromatography/quadrupole mass spectroscopy, Carol Stream 16 (2005) 65–120.

[55] T. Kim, B. Song, K.S. Cho, I.-S. Lee, Therapeutic potential of volatile terpenes and terpenoids from forests for inflammatory diseases, Int. J. Mol. Sci. 21 (2020) 2187, https://doi.org/10.3390/ijms21062187.

[56] Q.J. Wei, C.N. Wei, K. Harada, K. Minamoto, Y. Okamoto, M. Otsuka, A. Ueda, Evaluation of allergenicity of constituents of myoga using the murine local lymph node assay, Int. J. Immunopathol. Pharmacol. 23 (2010) 463–470, https://doi.org/10.1177/039463201002300208.

[57] M. Pesonen, S. Suomela, O. Kuuliala, M.-L. Henriks-Eckerman, K. Aalto-Korte, Occupational contact dermatitis caused by D-limonene, Contact Dermatitis 71 (2014) 273–279, https://doi.org/10.1111/cod.12287.

[58] S.H. Kim, S.Y. Lee, C.Y. Hong, K.S. Gwak, M.J. Park, D. Smith, I.G. Choi, Whitening and antioxidant activities of bornyl acetate and nezukol fractionated from Cryptomeria japonica essential oil, Int. J. Cosmet. Sci. 35 (2013) 484–490, https://doi.org/10.1111/ics.12069.

[59] S. Casiglia, M. Bruno, M. Bramucci, L. Quassinti, G. Lupidi, D. Fiorini, F. Maggi, Kundmannia sicula (L.) DC: a rich source of germacrene D, J. Essent. Oil Res. 29 (2017) 437–442, https://doi.org/10.1080/10412905.2017.1338625.

[60] H. Türkez, E. Aydın, In vitro assessment of cytogenetic and oxidative effects of α-pinene, Toxicol. Ind. Health 32 (2016) 168–176, https://doi.org/10.1177/0748233713498456.

[61] S.S. Dahham, Y.M. Tabana, M.A. Iqbal, M.B.K. Ahamed, M.O. Ezzat, A.S.A. Majid, A.M.S.A. Majid, The anticancer, antioxidant and antimicrobial properties of the sesquiterpene β-caryophyllene from the essential oil of aquilaria crassna, Molecules 20 (2015) 11808–11829, https://doi.org/10.3390/molecules200711808.

[62] F. Mollica, I. Gelabert, R. Amorati, Synergic antioxidant effects of the essential oil component γ-terpinene on high-temperature oil oxidation, ACS Food Sci. Technol. 2 (2022) 180–186, https://doi.org/10.1021/acsfoodscitech.1c00399.

[63] S. M, A. Te, In vitro antioxidant activity and scavenging effects of Cinnamomum verum leaf extract assayed by different methodologies, Food Chem. Toxicol. Int. J. Publ. Br. Ind. Biol. Res. Assoc. 44 (2006), https://doi.org/10.1016/j.fct.2005.06.013.

[64] M. El Jemli, R. Kamal, I. Marmouzi, Z. Doukkali, E.H. Bouidida, D. Touati, R. Nejjari, L. El Guessabi, Y. Cherrah, K. Alaoui, Chemical composition, acute toxicity, antioxidant and anti-inflammatory activities of Moroccan Tetraclinis articulata L, J. Tradit. Complement. Med. 7 (2016) 281–287, https://doi.org/10.1016/j.jtcme.2016.06.006.

[65] Ü. Ündeğer, A. Başaran, G.H. Degen, N. Başaran, Antioxidant activities of major thyme ingredients and lack of (oxidative) DNA damage in V79 Chinese hamster lung fibroblast cells at low levels of carvacrol and thymol, Food Chem. Toxicol. 47 (2009) 2037–2043, https://doi.org/10.1016/j.fct.2009.05.020.

[66] M. Ramos, A. Beltrán, M. Peltzer, A.J.M. Valente, M. del C. Garrigós, Release and antioxidant activity of carvacrol and thymol from polypropylene active packaging films, LWT–Food Sci. Technol. 58 (2014) 470–477, https://doi.org/10.1016/j.lwt.2014.04.019.

[67] J. Rúa, P. del Valle, D. de Arriaga, L. Fernández-Álvarez, M.R. García-Armesto, Combination of carvacrol and thymol: antimicrobial activity against Staphylococcus aureus and antioxidant activity, Foodb. Pathog. Dis. 16 (2019) 622–629, https://doi.org/10.1089/fpd.2018.2594.

[68] K. Majouli, M. Besbes Hlila, A. Hamdi, G. Flamini, H. Ben Jannet, A. Kenani, Antioxidant activity and α-glucosidase inhibition by essential oils from Hertia cheirifolia (L.), Ind. Crops Prod. 82 (2016) 23–28, https://doi.org/10.1016/j.indcrop.2015.12.015.
[69] S.K. Panigrahy, R. Bhatt, A. Kumar, Targeting type II diabetes with plant terpenes: the new and promising antidiabetic therapeutics, Biologia (Bratisl.). 76 (2021) 241–254, https://doi.org/10.2478/s11756-020-00575-y.
[70] Y. Guillín, M. Cáceres, R. Torres, E. Stashenko, C. Ortiz, Effect of essential oils on the inhibition of biofilm and quorum sensing in Salmonella enteritidis 13076 and Salmonella typhimurium 14028, Antibiot. Basel Switz. 10 (2021) 1191, https://doi.org/10.3390/antibiotics10101191.
[71] A.C. Lim, S.G.H. Tang, N.M. Zin, A.M. Maisarah, I.A. Ariffin, P.J. Ker, T.M.I. Mahlia, Chemical composition, antioxidant, antibacterial, and antibiofilm activities of Backhousia citriodora essential oil, Mol. Basel Switz. 27 (2022) 4895, https://doi.org/10.3390/molecules27154895.
[72] D. Sateriale, G. Forgione, G.A. De Cristofaro, C. Pagliuca, R. Colicchio, P. Salvatore, M. Paolucci, C. Pagliarulo, Antibacterial and antibiofilm efficacy of thyme (Thymus vulgaris L.) essential oil against foodborne illness pathogens, Salmonella enterica subsp. enterica Serovar typhimurium and Bacillus cereus, Antibiot. Basel Switz. 12 (2023) 485, https://doi.org/10.3390/antibiotics12030485.
[73] J. Monteiro Marques, S. Serrano, H. Selmi, P. Giesteira Cotovio, T. Semedo-Lemsaddek, Antimicrobial and antibiofilm potential of Thymus vulgaris and Cymbopogon flexuosus essential oils against pure and mixed cultures of foodborne bacteria, Antibiotics 12 (2023) 565, https://doi.org/10.3390/antibiotics12030565.